DEVELOPMENT OF A LINEAR ION TRAP FOR QUANTUM COMPUTING

D. M. LUCAS
Centre for Quantum Computation,
Clarendon Laboratory, Parks Road, Oxford OX1 3PU, U.K.
E-mail: d.lucas@physics.ox.ac.uk

We describe the latest work in our programme to implement a linear ion trap quantum information processor with $^{40}Ca^{+}$. This is an experimental demonstration of read-out for a qubit which is stored in the spin state of the valence electron, in the ground electronic level.

1 Introduction

Since the original suggestion of Cirac and Zoller,[1] the linear ion trap has been widely regarded as one of the most promising systems for the experimental implementation of quantum computing, at least on the scale of $\sim$10 qubits.[2,3] The isolated environment of an ion trap provides extremely good protection against decoherence[4] and motional degrees of freedom may be used to implement quantum logic gates.[5]

We have built a linear ion trap for $^{40}Ca^{+}$, with the aim of experiments in quantum information processing. $^{40}Ca^{+}$ is a promising ion species because it offers a moderately high recoil energy, yet the relevant transitions are accessible to solid-state diode lasers. In this paper we report a demonstration of state read-out for a qubit stored in the two Zeeman states of the ground $S_{1/2}$ level of this ion.

2 Quantum computing in $^{40}Ca^{+}$

The low-lying energy levels of $^{40}Ca^{+}$ are shown in figure 1(a). A natural choice for a pair of internal states to be used as a qubit are the $S_{1/2}^{\pm 1/2}$ Zeeman states of the ground level (we use the notation $L_J^{M_J}$ to represent the Zeeman state M_J of the level J in the term L), split by an external magnetic field. Since they are in the ground level these states are extremely long-lived, and coherent control is possible using Raman transitions via an intermediate state far-detuned from one of the S$\leftrightarrow$P transitions. The two beams required can both be derived from one laser, with a precisely-controlled radio-frequency splitting between them applied using acousto- or electro-optical techniques; thus the difficulties of addressing a very narrow transition directly are avoided. The Raman transition would also be used for cooling to the motional ground state, using sideband cooling or the recently-proposed EIT cooling of Morigi *et al.*[6] An alternative choice of qubit in $^{40}Ca^{+}$ is implemented in ref.[7]

3 Read-out for a ground state qubit

The difficulty with using this "ground state" qubit occurs when it is necessary to read out the qubit state (for example, at the end of any applied quantum logic gates, or even to probe the motional state populations after sideband or EIT cooling). A technique which naturally suggests itself for detecting the state of a single ion with high efficiency is that of

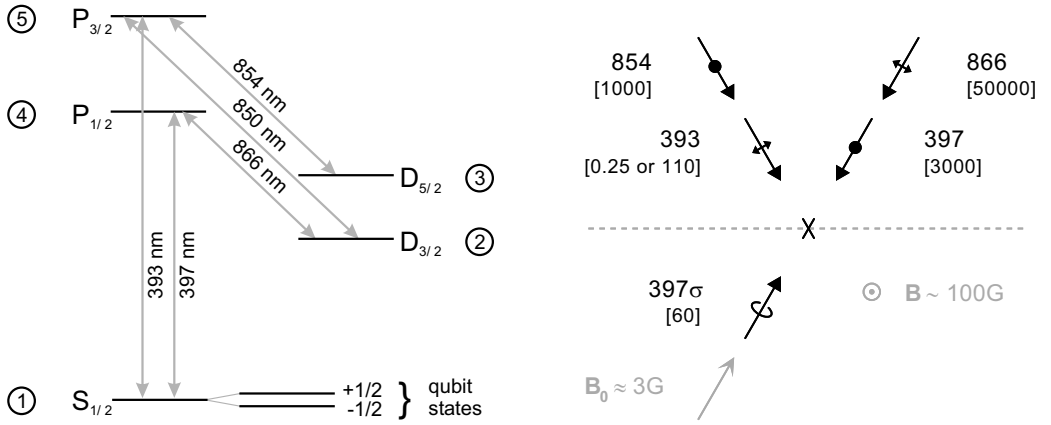

Figure 1. (a) Low-lying energy levels of $^{40}Ca^{+}$ with allowed transitions (wavelengths to the nearest nm). The proposed qubit states are indicated. The numbering of the levels is used in the text. (b) Directions and polarizations of laser beams in the experiment relative to the applied magnetic fields $\mathbf{B}$ (out of the page) and $\mathbf{B}_0$ where $\bullet$ represents linear polarization out of the page. Typical beam intensities (W/m^2) are indicated in brackets. The sense of the circular polarization of the 397σ beam is reversed between experimental runs. The position of the ion is indicated by $\times$ and the axis of the linear trap by the dashed line.

electron shelving.[8] In the present case this involves transferring the ion selectively from one of the qubit states to the metastable "shelved" $D_{5/2}$ level, where it will remain on average for $\tau(D_{5/2}) = 1168\,\mathrm{ms}$; if the near-resonant Doppler-cooling radiation on $S_{1/2} \leftrightarrow P_{1/2}$ is then applied (together with $D_{3/2} \leftrightarrow P_{1/2}$ repumping light) the ion will only fluoresce if it was *not* shelved. The presence or absence of fluorescence can be detected with high efficiency in a time short compared with $\tau(D_{5/2})$.

However, the splitting imposed between the $S_{1/2}^{\pm 1/2}$ Zeeman states should be small ($\sim$3 MHz), so as to minimize the effect of fluctuations in the applied magnetic field during coherent qubit manipulations. In this case the qubit states cannot be resolved from each other using the allowed S$\leftrightarrow$P transitions (which have linewidths $\approx 23\,\mathrm{MHz}$). Therefore we increase the magnetic field for the read-out phase of the experiment until the Zeeman components of these transitions are spectrally resolved. We may then shelve the $S_{1/2}^{-1/2}$ qubit state by exciting the 393 nm cycling transition $S_{1/2}^{-1/2} \leftrightarrow P_{3/2}^{-3/2}$ with a short pulse of σ^- polarized light, which allows spontaneous decay into the shelved level; due to a favourable $D_{5/2}/D_{3/2}$ branching ratio, the ion is shelved in $D_{5/2}$ with about 89% probability. Provided that the magnetic field is large enough that off-resonant excitation of the $S_{1/2}^{+1/2} \leftrightarrow P_{3/2}^{-1/2}$ transition is negligible, the $S_{1/2}^{+1/2}$ qubit state will be unaffected. Although not exploited in the present experiments, the 11% population 'lost' to $D_{3/2}$ could be recycled without corrupting the qubit state by applying subsequent pulses of 850 nm light on the $D_{3/2}^{-1/2} \leftrightarrow P_{3/2}^{-3/2}$ and $D_{3/2}^{-3/2} \leftrightarrow P_{3/2}^{-3/2}$ transitions; after several complete cycles the probability of $S_{1/2}^{-1/2}$ being shelved in $D_{5/2}$ would then be extremely close to 1.

A simplified rate equation solution for the population transfer during the 393 nm shelving pulse may be found analytically[9] by modelling the system as three levels $[S_{1/2}^{+1/2}, S_{1/2}^{-1/2}, D]$ with populations $[N_+(t), N_-(t), N_D(t)]$ respectively, and two transition rates: (i) the (de-

sired) rate R of transfer from $S_{1/2}^{-1/2}$ to the metastable D states, and (ii) the (undesired) rate R' of transfer from $S_{1/2}^{+1/2}$ to $S_{1/2}^{-1/2}$. Thus

$$\frac{\mathrm{d}}{\mathrm{d}t}N_+ = -R'N_+ \quad ; \quad \frac{\mathrm{d}}{\mathrm{d}t}N_- = R'N_+ - RN_- \quad ; \quad \frac{\mathrm{d}}{\mathrm{d}t}N_D = RN_-$$

where the initial condition $N_-(0) = 1 - N_+(0)$ is given (for example, $N_-(0) = 0.75$ if the ion is prepared in the $S_{1/2}^{-1/2}$ state in 75% of experiments) and $N_D(0) = 0$. The experiment measures the proportion N_3 of the population shelved in $D_{5/2}$, which we find to be

$$N_3(t) = bN_D(t) = \frac{bR}{R-R'}\left\{\left[N_-(0) - \frac{R'}{R}\right](1-\mathrm{e}^{-Rt}) + [1-N_-(0)](1-\mathrm{e}^{-R't})\right\} \qquad (1)$$

where the branching ratios give the numerical factor $b \approx 0.89$ and $t = \tau_{393}$ is the duration of the shelving pulse.

R occurs through resonant excitation of the $S_{1/2}^{-1/2} \leftrightarrow P_{3/2}^{-3/2}$ transition, to which the 393 nm laser is tuned, followed by spontaneous decay to the D states:

$$R = \frac{\Omega_{15}^2}{2\Omega_{15}^2 + \Gamma_5^2}(\Gamma_{25} + \Gamma_{35})$$

where the subscripts refer to levels numbered as in figure 1(a); Γ_{25}, Γ_{35} are the $P_{3/2} \rightarrow D_{3/2}, D_{5/2}$ spontaneous decay rates, and $\Gamma_5 = \sum_i \Gamma_{i5}$ is the reciprocal of the $P_{3/2}$ lifetime. The $S_{1/2} \leftrightarrow P_{3/2}$ Rabi frequency Ω_{15} is related to the $\lambda = 393\,\mathrm{nm}$ σ^- laser intensity I_{15} by

$$\Omega_{15}^2 = \frac{3\lambda^3\Gamma_5}{2\pi hc}I_{15}$$

R' arises from off-resonant excitation of $S_{1/2}^{+1/2} \rightarrow P_{3/2}^{-1/2}$ followed by spontaneous decay to $S_{1/2}^{-1/2}$:

$$R' = \frac{\pi}{9}\Omega_{15}^2\left(\frac{\Gamma_5/2\pi}{\delta^2 + \Gamma_5^2/4}\right)$$

where the detuning $\delta = \frac{2}{3}\mu_B B/\hbar$ and B is the magnetic field applied during the read-out pulse. These expressions allow the measured $D_{5/2}$ population $N_3(\tau_{393})$ to be related to the basic experimental parameters τ_{393}, B, I_{15} and $N_-(0)$.

Following ref.[9] we define the efficiency of the read-out process to be the difference between the shelved population $N_3(t)$ when $N_-(0) = 1$ and that when $N_-(0) = 0$. However, we allow for imperfect preparation of the initial populations and find that, in two experiments where the initial populations are $N_-^{(1)}(0)$ and $N_-^{(2)}(0)$, the observed efficiency is reduced by a factor $[N_-^{(1)}(0) - N_-^{(2)}(0)]$, to give

$$\epsilon(t) = \left[N_-^{(1)}(0) - N_-^{(2)}(0)\right]\frac{bR}{R-R'}\left(\mathrm{e}^{-R't} - \mathrm{e}^{-Rt}\right) \qquad (2)$$

with $N_-^{(1)}(0) > N_-^{(2)}(0)$. For the purposes of testing the read-out scheme, we attempt to ensure that $N_-^{(1)}(0) \approx 1$ and $N_-^{(2)}(0) \approx 0$.

4 Experiment

Much of the apparatus has already been described elsewhere.[10] We give here a brief review and details of the additions necessary for the present experiment.

4.1 Trap

The central vacuum chamber is evacuated to around 2×10^{-11} torr and a cloud of calcium ions is loaded into the linear Paul trap using a calcium oven and electron gun. After loading, the amplitudes of the radio-frequency (6.2 MHz) radial trapping field and the DC axial field are reduced to approximately $100\,V_{PP}$ and 30 V respectively (giving typical trap secular frequencies of 500 kHz radially and 200 kHz axially). A low-voltage "tickle" oscillation is then applied to one of the end-caps until only a single ion remains in the trap.

4.2 Lasers

Figure 1(b) shows the directions and polarizations of the various laser beams used in the experiment, relative to the low ($B_0 \approx 3\,G$) and high ($B \sim 100\,G$) applied magnetic fields. Typical intensities are also shown; beam spot sizes at the trap are $\sim 100 \times 100\,\mu m$. All five beams may be independently switched, either with mechanical shutters or with acousto-optic modulators. The lasers are of the external cavity grating-stabilized design, and all except the laser at 854 nm are locked to stabilized reference cavities which reduce linewidth and medium-term frequency drift to the 1 MHz level.

The 397 beam for Doppler cooling (to ~ 1 mK) and fluorescence detection is provided by a frequency-doubled master-slave diode system operating at 794 nm. The same laser system is used for the low-intensity 397σ beam whose circular polarization with respect to $\mathbf{B}_0$ is chosen to prepare the ion in either the $S_{1/2}^{+1/2}$ or $S_{1/2}^{-1/2}$ qubit state.

Light from a violet laser diode (393 beam) is used to transfer the ion from the $S_{1/2}^{-1/2}$ ground state to the shelved $D_{5/2}$ level, via $P_{3/2}^{-3/2}$. The intensity at the ion is very low since only ~ 50 transitions are necessary to shelve the ion, and the beam is switched using an AOM in order to give a shelving pulse of well-controlled duration (from 1 μs to 50 ms). The light is linearly-polarized perpendicular to the read-out magnetic field $\mathbf{B}$ and thus half the total beam intensity is available to excite any of the resolved σ components of the $S_{1/2} \leftrightarrow P_{3/2}$ transition; here it is tuned to be resonant with the $S_{1/2}^{-1/2} \leftrightarrow P_{3/2}^{-3/2}$ component.

The 866 repumping beam is polarized such that it repumps from all $D_{3/2}^{M_J}$ states, in both the low and high magnetic fields. The 854 beam is used to de-shelve the ion, after the detection phase, in preparation for the next experimental sequence.

4.3 Magnetic fields

The direction of the low field $\mathbf{B}_0$ is aligned parallel to the 397σ optical pumping beam by minimizing the ionic fluorescence due to the 397σ light. For practical reasons, the high field $\mathbf{B}$ is applied perpendicular to $\mathbf{B}_0$, so that the axis of the $S_{1/2}^{\pm 1/2}$ qubit states must be adiabatically rotated as $\mathbf{B}$ is applied. This is ensured by the ≈ 5 ms switch-on time-constant of the high-field coils; numerical simulations showed this to be at least an order of magnitude slower than the rate required to introduce a 1% error in the measured state.

4.4 Detection

Fluorescence from the ion at 397 nm is collected in a direction perpendicular to the plane of propagation of the laser beams by a compound lens which subtends a solid angle of 0.20 sr at the trap, and is imaged via a violet filter onto a photomultiplier connected to a gated photon counter. The net count rate from a single ion is around 30 kHz; a counting bin

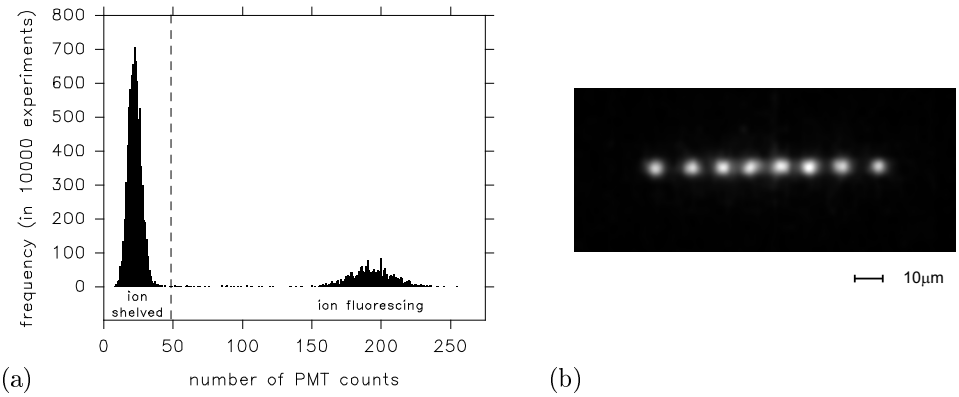

Figure 2. Detection methods. (a) Histogram of photomultiplier counts recorded during the 8 ms detection phase of 10,000 experimental sequences (section 4.5) in which a single ion was first optically pumped towards the $S_{1/2}^{-1/2}$ state, then shelved in the $D_{5/2}$ level as described in the text. The counts when the ion is shelved are due to scattered light from the 397 nm detection beam. A threshold (dashed line) is set to determine the number of experiments in which the ion was shelved; in this data set, the fluorescence is below the threshold in 80% of the experiments ($N_3 = 0.80$). (b) Linear crystal of eight ions, imaged on the intensified CCD camera. The camera provides spatial information, but this particular device does not possess sufficient quantum efficiency at 397 nm to detect whether individual ions are fluorescing or not as rapidly as the PMT.

of 8 ms gives ample discrimination between the "ion fluorescing" and "ion shelved" states, figure 2(a). An intensified CCD camera may alternatively be used for detection, for imaging ion crystals such as that in figure 2(b); in the experiments described here the camera is used only to check for the presence of non-fluorescing (*i.e.* non-$^{40}Ca^{+}$) ions.

4.5 Experimental sequence

To make a single read-out measurement, the following sequence of events occurs (where • indicates 'on'):

Action	*Duration*	*Laser beams*					*Magnetic fields*	
	(approx.)	397	397σ	393	854	866	**B**	$\mathbf{B}_0$
Doppler cooling	15 ms	•				•		•
Optical pumping	10 ms		•			•		•
Adiabatic rotation	30 ms					•	ramping	•
Shelving	1 μs–50 ms			•		•	•	•
Detection	8 ms	•				•		•
De-shelving	2 ms	•			•	•		•

This sequence is repeated many (typically 1000) times to obtain a measurement of the mean $D_{5/2}$ population. The read-out efficiency is deduced by comparing the $D_{5/2}$ population measured when the ion is prepared in the $S_{1/2}^{-1/2}$ state with that when it is prepared in $S_{1/2}^{+1/2}$.

The length τ_{393} of the shelving pulse depends on the intensity of the 393 nm laser beam; two different intensity regimes were investigated, with $\tau_{393} \sim 10$ ms at the lower intensity and $\tau_{393} \sim 10\,\mu$s at the higher one. The total length of the sequence is approximately (90 ms + τ_{393}), when the opening and closing delays of mechanical shutters are included.

The de-shelving phase ensures the ion is returned immediately to the cooling cycle, to avoid having to wait $\sim 1\,\mathrm{s}$ for it to decay spontaneously. The photon counter is gated on for 8 ms during the detection phase, to determine if the ion is shelved or not; and again during the Doppler cooling phase, to check that the ion returned correctly to the cooling cycle after the previous sequence.

5 Results

Results for the shelving efficiency as a function of shelving pulse duration τ_{393} are shown in figure 3. Figure 3(a) shows the measured $\mathrm{D}_{5/2}$ population, where each point represents 1000 experimental sequences. For each value of τ_{393} two runs were carried out, with the sense of the circular polarization of the 397σ beam reversed between them so as to prepare the initial population $N_-(0)$ predominantly in either $\mathrm{S}_{1/2}^{-1/2}$ or $\mathrm{S}_{1/2}^{+1/2}$. The data are fitted by equation 1 where the parameters I_{15} (393 nm σ^- intensity), $N_-^{(1)}(0)$ (for $397\sigma^-$ runs) and $N_-^{(2)}(0)$ (for $397\sigma^+$ runs) are simultaneously floated. The experiment differs slightly from the situation treated in section 3, in that the 866 nm repumping laser is left on during the shelving pulse which prevents any population ending up in the $\mathrm{D}_{3/2}$ level; to a first approximation this recycles about half the lost population back into $\mathrm{D}_{5/2}$ via the qubit state that is being read out ($\mathrm{S}_{1/2}^{-1/2}$) and we use a modified branching ratio $b = 0.94$ in equations 1 and 2.

The observed efficiency ϵ is the difference between the two data sets and is shown in figure 3(b), together with the fitted curve. At the optimum shelving pulse length of around 6 ms the efficiency reaches 60%. Also shown is the ideal efficiency that would be obtained if the initial state preparation were perfect. In a second experiment a higher intensity 393 nm shelving pulse was used, giving a peak observed read-out efficiency of 50% at $\tau_{393} \approx 15\,\mu\mathrm{s}$; the reduction in efficiency appeared to be due to poorer initial state preparation.

Figure 4 shows the shelving efficiency as a function of the magnetic field B applied for read-out, where τ_{393} was fixed at the optimum value of 6 ms. The data are again fitted by equation 1, with independent variable B and the same parameters floated as previously. The field strength was calibrated from the Zeeman shift of the $\mathrm{S}_{1/2}^{-1/2} \leftrightarrow \mathrm{P}_{3/2}^{-3/2}$ component.

Given the simplifications in the limited rate-equation treatment, the fits are satisfactory, and indicate 10–15% imperfection in the state preparation and a 393 nm σ^- intensity at the ion of 40–60% of the measured beam intensity in this polarization (implying the beam was not perfectly centred on the ion). We do not account for residual Doppler broadening or laser linewidth, which are small ($\sim$1 MHz) compared to the $\mathrm{S}_{1/2} \leftrightarrow \mathrm{P}_{3/2}$ natural width.

6 Discussion and Prospects

As discussed by Stevens *et al.*,[9] read-out efficiencies significantly less than 100% do not necessarily render quantum computations inefficient and the main cost is the need to re-run an algorithm several times; from figures 3(a) and 4(a) the two different initial states can clearly be discriminated (even when $\epsilon < 50\%$), and could be with significantly less repetitions than the 1000 used here, with optimized parameters.

The observed efficiency of this read-out method appears to be limited mainly by imperfect optical pumping used to prepare the initial states; we have no reason to doubt that with correctly-prepared initial populations the read-out efficiency would approach its theoretical optimum at large magnetic field, or that it could be made close to 100% by repumping

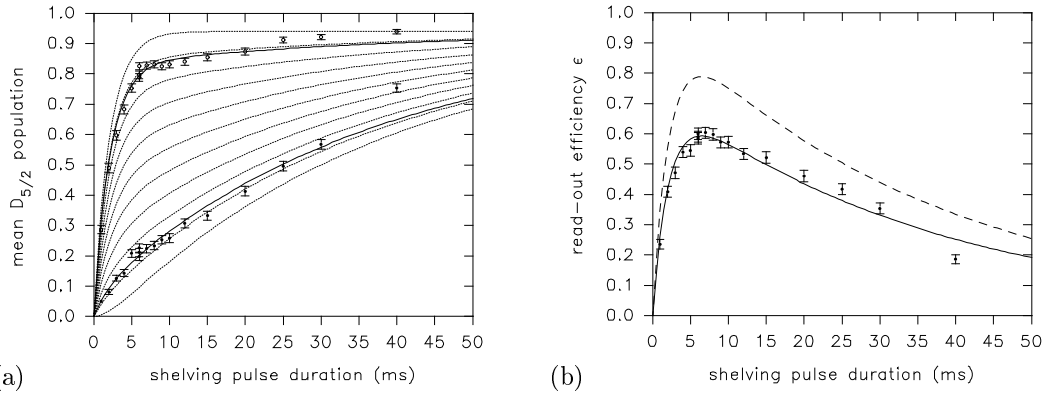

Figure 3. Read-out efficiency as a function of the duration τ_{393} of the 393 nm $S_{1/2}^{-1/2} \rightarrow P_{3/2}^{-3/2}$ shelving pulse, for fixed magnetic field $B = 98\,\mathrm{G}$. Error bars are statistical. (a) Mean $D_{5/2}$ population at the end of the shelving pulse, for a single ion previously pumped with 397 nm σ^- light (○) or 397 nm σ^+ light (●). Each data point represents 1000 experimental sequences. The fit from equation 1 (solid lines) gives $N_-^{(1)}(0) = 0.89(1)$, $N_-^{(2)}(0) = 0.13(1)$, $I_{15} = 0.054(3)\,\mathrm{W/m^2}$. The measured 393 nm σ^- intensity was estimated to be $0.12(4)\,\mathrm{W/m^2}$ at the centre of the beam. The dotted lines show the predictions of the theory for $N_-(0) = 0 \ldots 1$ in ten steps. (b) Observed read-out efficiency ϵ for the same data. The solid line is equation 2 with the above parameters. The dashed line shows the expected efficiency if the initial populations had been perfectly prepared, that is, if $N_-^{(1)}(0) - N_-^{(2)}(0) = 1$.

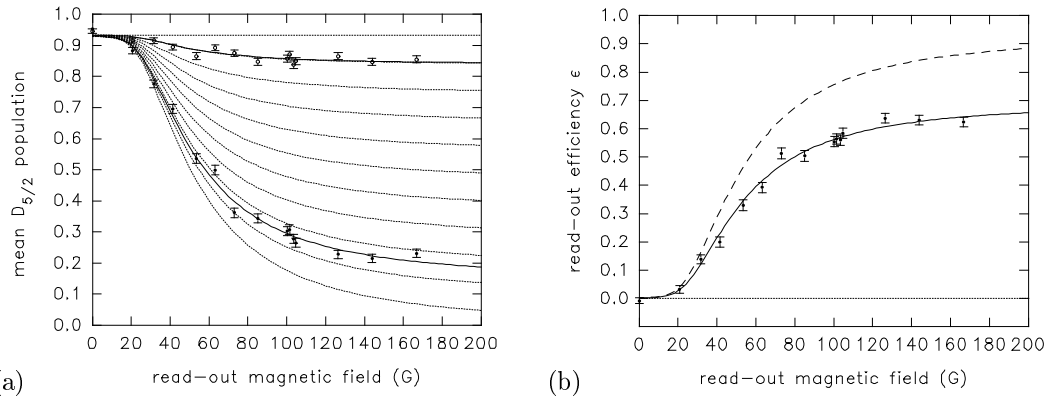

Figure 4. Shelving efficiency as a function of the read-out magnetic field B, for fixed shelving pulse duration $\tau_{393} = 6$ ms. Error bars are statistical. (a) Mean $D_{5/2}$ population at the end of the shelving pulse, for a single ion previously pumped with 397 nm σ^- light (○) or 397 nm σ^+ light (●). Each data point represents 1000 experimental sequences. The fit from equation 1 (solid lines) gives $N_-^{(1)}(0) = 0.90(1)$, $N_-^{(2)}(0) = 0.16(1)$, $I_{15} = 0.091(3)\,\mathrm{W/m^2}$. The measured 393 nm σ^- intensity was estimated to be $0.15(5)\,\mathrm{W/m^2}$ at the centre of the beam. The dotted lines show the predictions of the theory for $N_-(0) = 0 \ldots 1$ in ten steps. (b) Observed read-out efficiency ϵ for the same data. The solid line is equation 2 with the above parameters. The dashed line shows the expected efficiency if the initial populations had been perfectly prepared, that is, if $N_-^{(1)}(0) - N_-^{(2)}(0) = 1$.

from $D_{3/2}$ with 850 nm light as mentioned in section 3. The limited state preparation efficiency is probably due to the switching of the high magnetic field necessary in this scheme: at constant low field we obtain very efficient optical pumping (a reduction of the 397 nm fluorescence from an intense 397σ beam by a factor > 50), but when the high magnetic field is switched at $\sim$10 Hz as in the read-out experiments the optical pumping is much less efficient (the fluorescence observed during the low-field optical pumping pulse is reduced by a factor ~ 4 only). By varying the direction of the low magnetic field with respect to the optical pumping beam during sequences of read-out experiments we were unable to improve the shelving efficiency, implying that the problem is due to fluctuating transient fields; the fluorescence observed indicates these are at the $\sim$1 G level.

Although it might be possible to reduce these magnetic field transients, they will be a more serious problem when it comes to manipulation of the qubit states themselves by driving Raman transitions between them. Then the energy separation of the qubit states, which is first-order dependent on the magnetic field, must be kept constant, leading to a requirement on the magnetic field stability at the mG level. Hence we are currently investigating the possibility of alternative laser read-out methods which do not require the magnetic field to be increased, but still avoid the need for sophisticated laser stabilization.

One such method is to excite Raman transitions $S_{1/2}^{+1/2} \leftrightarrow (P_{1/2}^{-1/2}) \leftrightarrow D_{3/2}^{+1/2}$ followed by spontaneous scattering on the $D_{3/2}^{+1/2} \leftrightarrow P_{3/2}^{+3/2}$ transition to shelve the $S_{1/2}^{+1/2}$ qubit state in $D_{5/2}$; here the selection of Zeeman states is achieved by polarization rather than large magnetic fields. A second possibility is to shelve using the $S_{1/2} \leftrightarrow P_{3/2}$ transition again, but to use electromagnetically-induced transparency to suppress the $S_{1/2}^{-1/2} \leftrightarrow P_{3/2}^{+1/2}$ transition whilst allowing the $S_{1/2}^{+1/2} \leftrightarrow P_{3/2}^{+3/2}$ transition, for example; here a second, relatively intense, pump laser operating close to the $D_{3/2} \leftrightarrow P_{3/2}$ transition is used to provide the EIT. Preliminary calculations suggest that this second scheme can produce a read-out efficiency close to 90% with lasers stabilized to the 1 MHz level and with 1% polarization impurity.

Acknowledgments

None of the work described would have been possible without present and past members of the Oxford ion-trapping group, Paul Barton, Charles Donald, Matt McDonnell, Derek Stacey, J.-P. Stacey, Andrew Steane and David Stevens, or the technical assistance of Graham Quelch. The research is supported by the EPSRC and Christ Church, Oxford.

References

1. J. I. Cirac and P. Zoller, Phys. Rev. Lett. **74**, 4091 (1995).
2. A. M. Steane, Appl. Phys. B **64**, 632 (1996).
3. C. Monroe *et al.*, Phys. Rev. A **55**, R2489 (1997).
4. R. J. Hughes *et al.*, Phys. Rev. Lett. **77**, 3240 (1996).
5. C. Monroe *et al.*, Phys. Rev. Lett. **75**, 4714 (1995).
6. G. Morigi, J. Eschner and Ch. Keitel, Phys. Rev. Lett. **85**, 4458 (2000).
7. H. C. Nägerl *et al.*, Phys. Rev. A **61**, 023405 (2000).
8. W. Nagourney, J. Sandberg and H. Dehmelt, Phys. Rev. Lett. **56**, 2797 (1986).
9. D. Stevens, J. Brochard and A. Steane, Phys. Rev. A **58**, 2750 (1998).
10. P. A. Barton *et al.*, Phys. Rev. A **62**, 032503 (2000).